Inorg. Chem. **2008**, *47*, 10184−10186

A $[Mn^{III}_3O]^{7+}$ Single-Molecule Magnet: the Anisotropy Barrier Enhanced by Structural Distortion

Chen-I Yang,[†] Wolfgang Wernsdorfer,[‡] Kai-Hung Cheng,[†] Motohiro Nakano,[§] Gene-Hsiang Lee,[||] and Hui-Lien Tsai*,[†]

Department of Chemistry, National Cheng Kung University, Tainan 701, Taiwan, Republic of China, Institut Néel, CNRS & UJF, BP-166, 25 Avenue des Martyrs, 38042 Grenoble Cedex 9, France, Division of Applied Chemistry, Graduate School of Engineering, Osaka University, 2-1 Yamada-oka, Suita 565-0871, Japan, and Instrumentation Center, College of Science, National Taiwan University, Taipei 106, Taiwan, Republic of China

Received July 2, 2008

A trinuclear manganese complex, $[Mn_3O(Me\text{-}salox)_3(2,4'\text{-}bpy)_3(ClO_4)]\cdot 0.5MeCN$ (**1**·0.5MeCN; Me-H_2salox = 2-hydroxyphenylethanone oxime), has been synthesized and characterized structurally as a $[Mn^{III}_3(\mu_3\text{-}O)]^{7+}$ core. Structural distortion by the twisting of the oxime ligand dominates ferromagnetic interactions within three Mn ions to give an $S = 6$ ground state as well as to enhance the anisotropy barrier U_{eff} to 37.5 K.

Some manganese clusters have received considerable interest in recent years because of their special magnetic properties so-called as single-molecule magnets (SMMs), which represent nanoscale magnetic particles with a well-defined size.[1,2] The remarkable magnetic properties of an SMM arise from its high-spin ground state (S) split by a large negative axial zero-field splitting (D), which results in an anisotropy energy barrier of about $U = |D|S_z^2$.[3] SMMs display sluggish magnetization relaxation phenomena such as magnetization hysteresis loops and frequency-dependent out-of-phase alternating current (ac) magnetic susceptibilities.[4] Recent research has focused on raising the effective barrier (U_{eff}) to reorientatation of the magnetization by increasing the molecule size up to Mn_{84} and the spin values up to $S = {}^{83}/_2$.[5] A record barrier of $U_{eff} = 86$ K was achieved for a Mn_6 complex.[5d] New applications to molecule spintronics have also been reported.[5e]

Compounds containing high-spin Mn^{III} ions are magnetically interesting because of their pronounced magnetic anisotropies provided by the Jahn−Teller (JT) distortions. Thus, many current routes to SMMs culminate in manganese(III)-containing complexes, to achieve the associated large single-ion anisotropy.[6] Trinuclear complexes with a $[Mn_3O]^{7+}$ core structure have been explored;[7] however, only a few examples of $[Mn_3O(O_2CR)_3(mpko)_3](ClO_4)$ (R = Me, Et, and Ph) with anisotropy barrier $U_{eff} \sim 10$ K and $[Mn_3O(^tBu\text{-}sao)_3Cl(MeOH)_5]$ have been presented as SMMs.[8] We herein reported a new $[Mn_3O]^{7+}$

* To whom correspondence should be addressed. E-mail: hltsai@mail.ncku.edu.tw.
[†] National Cheng Kung University.
[‡] Institut Néel, CNRS & UJF.
[§] Osaka University.
[||] National Taiwan University.

(1) Aromi, G.; Brechin, E. K. *Struct. Bonding (Berlin)* **2006**, *122*, 1.
(2) (a) Christou, G.; Gatteschi, D.; Hendrickson, D. N.; Sessoli, R. *MRS Bull.* **2000**, *25*, 66. (b) Gatteschi, D.; Sessoli, R. *Angew. Chem., Int. Ed.* **2003**, *42*, 268.
(3) Mirebeau, I.; Hennion, M.; Casalta, H.; Andres, H.; Güdel, H. U.; Irodova, A. V.; Caneschi, A. *Phys. Rev. Lett.* **1999**, *83*, 628.
(4) (a) Friedman, J. R.; Sarachik, M. P.; Tejada, J.; Ziolo, R. *Phys. Rev. Lett.* **1996**, *76*, 3830. (b) Wernsdorfer, W.; Sessoli, R. *Science* **1999**, *284*, 133.
(5) (a) Castro, S. L.; Sun, Z.; Grant, C. M.; Bollinger, J. C.; Hendrickson, D. N.; Christou, G. *J. Am. Chem. Soc.* **1998**, *120*, 2365. (b) Tasiopoulos, A. J.; Vinslava, A.; Wernsdorfer, W.; Abboud, K. A.; Christou, G. *Angew. Chem., Int. Ed.* **2004**, *43*, 2117, and references cited therein. (c) Ako, A. K.; Hewitt, I. J.; Mereacre, V.; Clérac, R.; Wernsdorfer, W.; Anson, C. E.; Powell, A. K. *Angew. Chem., Int. Ed.* **2006**, *45*, 4926. (d) Milios, C. J.; Vinslava, A.; Wernsdorfer, W.; Moggach, S.; Parsons, S.; Perlepes, S. P.; Christou, G.; Brechin, E. K. *J. Am. Chem. Soc.* **2007**, *129*, 2754. (e) Bogani, L.; Wernsdorfer, W. *Nat. Mater.* **2008**, *7*, 179.
(6) (a) Boskovic, C.; Wernsdorfer, W.; Folting, K.; Huffman, J. C.; Hendrickson, D. N.; Christou, G. *Inorg. Chem.* **2002**, *41*, 5107. (b) Milios, C. J.; Vinslava, A.; Wernsdorfer, W.; Moggach, S.; Parsons, S.; Perlepes, S. P.; Christou, G.; Brechin, E. K. *J. Am. Chem. Soc.* **2007**, *129*, 2754. (c) Yang, C.-I.; Wernsdorfer, W.; Tsai, Y.-J.; Chung, G.; Kuo, T.-S.; Lee, G.-H.; Shieh, M.; Tsai, H.-L. *Inorg. Chem.* **2008**, *47*, 1925.
(7) (a) Vincent, J. B.; Chang, H. R.; Folting, K.; Huffman, J. C.; Christou, G.; Hendrickson, D. N. *J. Am. Chem. Soc.* **1987**, *109*, 5703, and references cited therein. (b) McCusker, J. K.; Jang, H. G.; Wang, S.; Christou, G.; Hendrickson, D. N. *Inorg. Chem.* **1992**, *31*, 1874. (c) Jones, L. F.; Rajaraman, G.; Brockman, J.; Murugesu, M.; Raftery, J.; Teat, S. J.; Wernsdorfer, W.; Christou, G.; Brechin, E. K.; Collison, D. *Chem.—Eur. J.* **2004**, *10*, 5180. (d) Milios, C. J.; Wood, P. A.; Parsons, S.; Foguet-Albiol, D.; Lampropoulos, C.; Christou, G.; Perlepes, S. P.; Brechin, E. K. *Inorg. Chim. Acta* **2007**, *360*, 3932.
(8) (a) Stamatatos, T. C.; Foguet-Albiol, D.; Lee, S.-C.; Stoumpos, C. C.; Raptopoulou, C. P.; Terzis, A.; Wernsdorfer, W.; Hill, S. O.; Perlepes, S. P.; Christou, G. *J. Am. Chem. Soc.* **2007**, *129*, 9484. (b) Xu, H.-B.; Wang, B.-W.; Pan, F.; Wang, Z.-M.; Gao, S. *Angew. Chem., Int. Ed.* **2007**, *46*, 7388.

10.1021/ic8012238 CCC: $40.75 © 2008 American Chemical Society
Published on Web 10/11/2008

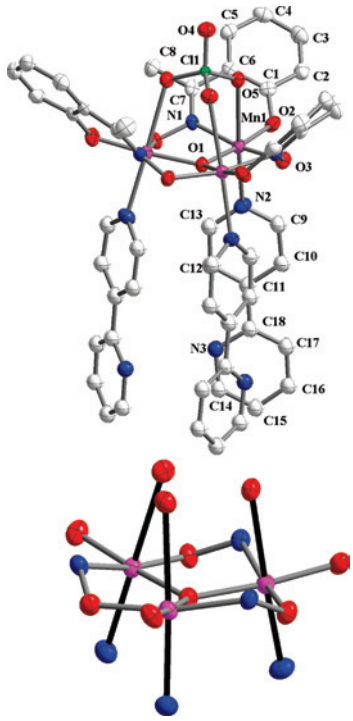

Figure 1. ORTEP drawings: (top) structure of **1**·0.5MeCN with thermal ellipsoids set at 30% probability; (bottom) side view of JT axes. The solid black lines describe those three JT axes. The solvent molecule H atoms have been omitted for clarity.

complex, in which the oxime ligand twisting makes the core distorted, and this distortion enhances the anisotropy barrier U_{eff} to 37.5 K.

The reaction of $Mn(ClO_4)_2 \cdot 6H_2O$ (1 equiv), 2,4′-bipyridine (2,4′-bpy; 1 equiv), and 2-hydroxyphenylethanone oxime (Me-H_2salox; 1 equiv) with NEt_3 (1 equiv) in MeCN formed a deep-brown solution, and this solution was slowly diffused by Et_2O to form dark-brown crystals of $[Mn_3O(Me\text{-salox})_3(2,4'\text{-bpy})_3(ClO_4)] \cdot 0.5MeCN$ (**1**·0.5MeCN) in yield of 38%.[9]

Complex **1**·0.5MeCN crystallizes in trigonal space group $P\bar{3}$. The crystal structure of **1**[10] is shown in Figure 1, which consists of a typical near-equilateral Mn^{III}_3 triangle core connected by a μ_3-oxide (O1) on the central plane. This triangle is capped by one ClO_4^- ion on the upper plane in a rare $\eta^1{:}\eta^1{:}\eta^1{:}\mu_3$ mode. The C_3 axis is perpendicular to the Mn^{III}_3 plane and passes through O4 and Cl1 of ClO_4^- and the central O atom, which lies 0.28 Å below the plane defined by the three Mn ions. The core of complex **1** is similar to the core of $[Mn_3O(O_2CR)_3(mpko)_3](ClO_4)$ (R = Me, Et, and Ph), in contrast to the vast majority of triangular $[Mn_3(\mu_3\text{-}O)]^{6+/7+}$ species in which the central O ion and the metal ions are coplanar.[7] Each edge of the triangle is bridged by a dianionic oximate group of a Me-salox^{2-} ligand in the $\eta^1{:}\eta^1{:}\mu_2$ mode, whose deprotonated hydroxyl group is bound terminally to a Mn^{III} ion. The methyl group twists the

(9) Satisfactory elemental analytical data for $[Mn_3O(Me\text{-salox})_3(2,4'\text{-bpy})_3(ClO_4)] \cdot 0.5MeCN$. Found: C, 54.29; H, 4.06; N, 10.40. Calcd: C, 54.29; H, 3.85; N, 10.94.

(10) Crystal data for **1**·0.5MeCN, $C_{55}H_{46.5}ClMn_3N_{11}$, M = 1216.79, trigonal, $P\bar{3}$, a = 12.8734(6) Å, c = 18.3364(9) Å, V = 2631.7(2) Å^3, T = 150(2) K, Z = 2, d_{calc} = 1.536 mg m^{-3}, no. of indep reflns 4041 [R(int) = 0.0681], no. of data 4041, no. of parameters 242, R [$F > 2\sigma(F)$], R (R_w) = 0.0762 (0.1684).

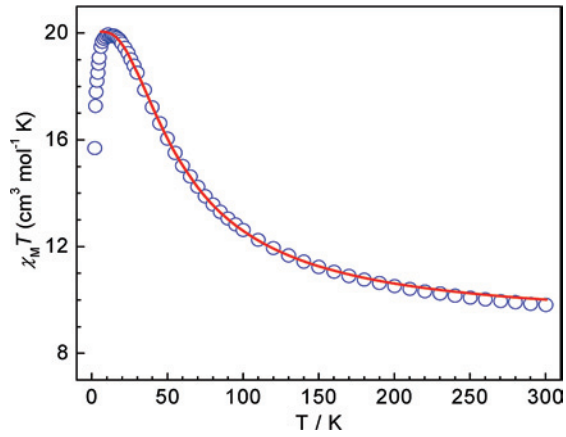

Figure 2. $\chi_M T$ vs T plot for **1**·0.5MeCN at 1000 G. The solid line represents a least-squares fit of the data.

Mn−N−O−Mn arrangement in a torsion angle of α_v = 44.15°. One N2 atom of the 2,4′-bipyridine ligand completes six-coordination at Mn1 and adopts a distorted octahedral geometry. The Mn^{III} oxidation state and O^{2-} protonation level were established by the bond valence sum (BVS) calculations,[11] the charge considerations, and the presence of a Mn^{III} JT elongation axis (O5−Mn1−N2). In addition, the JT axes of Mn^{III} ions are almost parallel to each other as well as to the crystallographic C_3 axis. The closest intermolecular Mn−Mn distance is ∼10 Å.

The variable-temperature direct current (dc) magnetic susceptibility data were collected for the powder sample of compound **1**·0.5MeCN in the temperature range of 2−300 K at a magnetic field of 1000 G (Figure 2). The value of $\chi_M T$ increases steadily from 9.81 cm^3 mol^{-1} K at 300 K as the temperature is lowered, to reach a maximum of 19.95 cm^3 mol^{-1} K at 11.0 K, and then decreases to 15.69 cm^3 mol^{-1} K at 2.0 K. The $\chi_M T$ value at 300 K is significantly larger than 9.00 cm^3 mol^{-1} K, the value expected for a Mn^{III}_3 complex with noninteracting metal centers with g = 2.0. This behavior clearly indicates the ferromagnetic coupling within **1**·0.5MeCN, and the small decrease in $\chi_M T$ at low temperature is likely the result of the Zeeman effect or zero-field splitting in the ground state. In order to describe the coupling within the cluster, the magnetic susceptibility data were fit to the appropriate χ_M vs T plot using a Mn^{III}_3 Heisenberg−van Vleck model (see Figure 1S in the Supporting Information). The data below 6.0 K were omitted in the fitting because zero-field splitting and the Zeeman effect dominate in this temperature range. The fitting result of dc data in 1000 G gave the best-fit parameters of g = 1.95 and J = 3.58 cm^{-1}. This set of parameters led to the result that S_T = 6, and the next state, S = 5, is close by at 43 cm^{-1}. It is noted that the ferromagnetic interactions between Mn ions in **1**·0.5MeCN may due to the twisting of the Mn−N−O−Mn arrangement in a torsion angle of 44.15°, for which similar results were recently reported.[12]

To investigate whether **1**·0.5MeCN might be a SMM, ac susceptibility measurements were performed in a 3.5 G ac field oscillating at 1−1488 Hz and with a zero applied dc

(11) (a) Brown, I. D.; Altermatt, D. *Acta Crystallogr., Sect. B* **1985**, *41*, 244. (b) Liu, W.; Thorp, H. H. *Inorg. Chem.* **1993**, *32*, 4102.

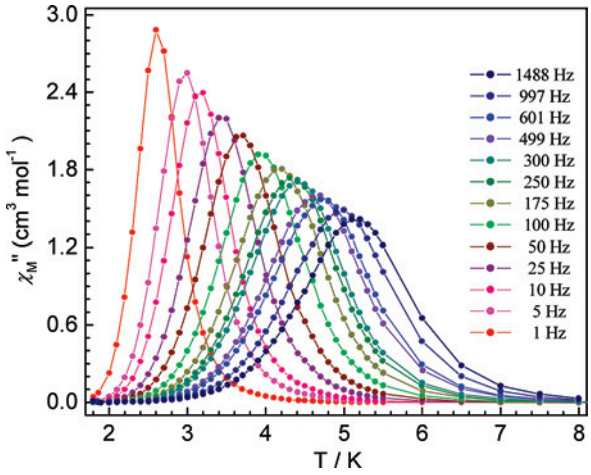

Figure 3. Plots of χ_M'' vs T for a microcrystalline sample of complex **1**·0.5MeCN in a 3.5 G ac field. The data were collected in an ac field oscillating at the indicated frequency.

field. The in-phase ($\chi_M'T$) signals showed a frequency-dependent decrease at $T = 6.5$ indicative of the onset of slow magnetic relaxation (Figure 5S in the Supporting Information). The out-of-phase (χ_M'') signals increased as the temperature was lowered, reaching a maximum value at 2.5−6.0 K followed by approaching zero, which was a frequency dependence. The plots of χ_M'' vs T are shown in Figure 3. As the frequency of the ac field was changed from 1488 to 1 Hz, the χ_M'' peak shifted from 5.1 to 2.6 K. This frequency dependence of the ac signals suggests that complex **1**·0.5MeCN is an SMM and is caused by the inability of **1**·0.5MeCN to relax quickly enough to keep up with the oscillating field at these temperatures.

To probe the anisotropy and quantum tunneling magnetization (QTM) of complex **1**·0.5MeCN, single-crystal hysteresis loops and relaxation measurements were performed by using a micro-SQUID setup.[13] The magnetization (M) vs H measurements are shown in Figure 4. Hysteresis loops were observed whose coercivity was strongly temperature- and sweep-rate-dependent, increasing with decreasing temperature and increasing field sweep rate, as is expected for the superparamagnetic-like behavior of a SMM. In addition, the hysteresis loops also show steps at regular intervals of the field indicative of QTM. Data obtained by varying the frequency of the oscillation of the ac field were fit to the Arrhenius equation to obtain the effective energy barrier (U_{eff}) for the relaxation of magnetization. Additional relaxation time measurements were obtained at temperatures below 2.6 K by the dc magnetization decay versus time measurements (Figure 4, bottom). This gave a set of relaxation time versus T data, which were combined with the ac data and used to construct an Arrhenius plot. The slope of the thermally activated region yielded an effective energy barrier for reorientation of the magnetization of U_{eff} of 37.5(2) K and $\tau_0 = 1.0 \times 10^{-7}$ s. Below 1.3 K, the relaxation

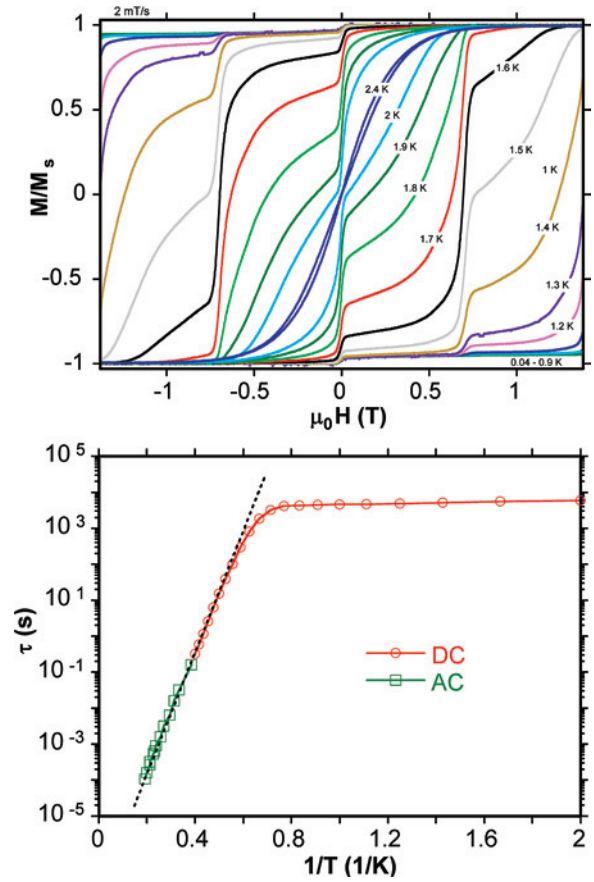

Figure 4. Magnetization hysteresis loops for a single crystal of **1**·0.5MeCN: (top) from 2.4 to 0.04 K at a 0.002 T s^{1-} scan rate; (bottom) Arrhenius plot using ac and dc data. The dashed line is the fit of the thermally activated region.

rate became almost temperature-independent, suggesting relaxation only via the ground-state quantum tunneling.

The first detailed study of the quantum steps suggests that the resonance at 0.7 T is due to a tunnel transition between states of the ground-state multiplet $S = 6$ and the first excited-state multiplet $S = 5$. The D value of $S = 6$ can be estimated from $D = g\mu_B\mu_0\Delta H \approx 1.3$ cm^{-1}, where ΔH is the field separation between the resonances at 0 and 1.45 T. The large D value would correspond to the almost parallel JT axes of the Mn^{III} ions.

In summary, we have described the synthesis, structure, and magnetic properties of a trinuclear $[Mn_3O]^{7+}$ complex. Magnetic studies indicate that complex **1**·0.5MeCN is a SMM with $S = 6$ and also a magnetic anisotropy barrier of $U_{eff} = 37.5$ K, which may due to the twisting of the Mn−N−O−Mn arrangement in a torsion angle of 44.15°.

Acknowledgment. The magnetic measurements were obtained from SQUID (MPMS XL-7) in NSYSU, and we thank the National Science Council of Taiwan (Grant NSC-96-2113-M-006-010-MY3) for financial support.

Supporting Information Available: Crystallographic details in CIF format, syntheses, crystallographic and BVS data, exchange pathway, χ_M^{-1} vs T plots, crystal packing, and magnetization hysteresis loops. This material is available free of charge via the Internet at http://pubs.acs.org.

IC8012238

(12) (a) Yang, C.-I.; Wernsdorfer, W.; Lee, G.-H.; Tsai, H.-L. *J. Am. Chem. Soc.* **2007**, *129*, 456. (b) Milios, C. J.; Vinslava, A.; Wernsdorfer, W.; Prescimone, A.; Wood, P. A.; Parsons, S.; Perlepes, S. P.; Christou, G.; Brechin, E. K. *J. Am. Chem. Soc.* **2007**, *129*, 6547.
(13) Wernsdorfer, W. *Adv. Chem. Phys.* **2001**, *118*, 99.